Discovery of Canine Drug Toceranib Phosphate as a Repurposed Agent against Human Hepatocellular Carcinoma

ling qiao
Chengdu University of TCM: Chengdu University of Traditional Chinese Medicine
Siyuan Qin
Sichuan University West China Hospital
Ningna Weng
Sichuan University West China Hospital
Bowen Li
Sichuan University West China Hospital
Maochao Luo
Sichuan University West China Hospital
Zhe Zhang
Sichuan University West China Hospital
Li Zhou
Sichuan University West China Hospital
Cen Jiang
Chengdu University of TCM: Chengdu University of Traditional Chinese Medicine
Canhua Huang (hcanhua@scu.edu.cn)
Sichuan University State Key Laboratory of Biotherapy

Research Article

Keywords: Hepatocellular carcinoma, Toceranib phosphate, Apoptosis, Autophagy

Posted Date: January 31st, 2022

DOI: https://doi.org/10.21203/rs.3.rs-1298194/v1

Abstract

Background

Human hepatocellular carcinoma (HCC) is an aggressive malignancy worldwide with a poor clinical outcome. There are limited therapeutic options currently available for those diagnosed with terminal HCC and therefore incorporating novel agents into standard-of-care regimens is urgently needed. In contrast to *de novo* drug discovery, the strategy of repurposing already-approved compounds initially designed to treat animals, which share similarities in disease-associated characteristics with humans (*i.e.*, dogs), might yield substantial advantages in terms of efficacy and safety. Given the evidence for clinical efficacy of toceranib phosphate (TOC) against canine carcinomas, we aimed to investigate its potential therapeutic effects on human HCC and the mechanisms involved.

Methods

We evaluated the antitumor effects of TOC using human HCC cell-line and cell line-derived xenograft models. Changes in autophagic response upon TOC exposure were quantified through immunoblotting and immunofluorescence analysis. The role of TOC-triggered autophagy was addressed via pharmacological and genetic inhibition.

Results

TOC, an approved canine drug, exhibited potent antitumor activity against human HCC cells by stimulating apoptosis *in vitro* and *in vivo*, which was accompanied by a concomitant increase in autophagic flux. Artificially blocking the TOC-triggered autophagy, either by pharmacologically using autophagy inhibitors or genetic interference, significantly inhibited cellular proliferation *in vitro* and decreased tumor burden *in vivo*, indicating a protective role of autophagy against TOC-mediated HCC cell death. This role played by TOC-induced autophagy was further linked to the inactivation of Akt/mTOR pathway that can be largely attributed to the upregulation of matricellular protein Cyr61 in HCC cells. Moreover, *in vivo* and *in vitro* treatment with standard systemic therapeutic sorafenib plus TOC resulted in pronounced synergistic effects on HCC cells.

Conclusions

Our results elucidate a newly identified therapeutic potential of TOC in treating HCC, sparking a growing interest in repurposing such canine drugs for human use.

1. Background

Multiple lines of evidence indicate that comparative oncology clinical trials using dogs as research models give acceptable knowledge under the explorations that can be conducted in the veterinary setting to solve specific obstacles in cancer therapy that cannot be completely solved in other traditional species (*e.g.*, mice) [1]. And in particular, dogs act as a sentinel in the aspect of etiology and epidemiology for the paradigm shift of human cancer development [2]. More specifically, canine cancers appear to precisely recapitulate the histopathology and biology of the corresponding human cancers, highlighting an immense value of comparative and translational studies for therapeutic benefits to both dogs and humans in need [3]. From the therapeutic point of view, existing canine drugs carry considerable important information regarding therapeutic responses and resistance patterns, which supports their incorporation into preclinical trials and in some ways enables new antineoplastic drugs to be born with an abbreviated trial-and-error process. Because of this, repurposing of canine drugs might mitigate part of the risk associated with development of entirely new drugs, providing us an alternative route to solve clinical dilemmas and achieve the ultimate goal of rapid application in patients with cancers. An encouraging sign is that these fundamental similarities between canine and human carcinomas seem to motivate a concern on agents targeting crucial pathways or molecular drivers shared by cancers in people and dogs. At this point, one of the earliest examples — RTK inhibitors toceranib and sunitinib can be drawn, which might inform the subsequent work with them or other selective TKI inhibitors for veterinary and human use [3,4].

Primary hepatocellular carcinoma (HCC) remains one of the leading malignancies globally characterized by high case-fatality rates and rising treatment costs, the incidence of which has reached a peak in recent years despite numerous advances in varied medical, locoregional and surgical therapies for HCC [5,6]. While these currently available approaches, such as surgical resection, orthotopic liver transplantation or local percutaneous tumor ablation, have truly benefited patients with early-stage HCC; a significant portion of patients diagnosed with advanced-stage disease are not surgical candidates and therefore starved of appropriate therapeutic options [5]. Despite signs of a promised and short-term improvement for those cases using standard-of-care regimens (*i.e.*, oral sorafenib), the majority of patients with late-stage HCC are confronted with unavoidable relapse or treatment discontinuity caused by *de novo* resistance or adverse reactions [7,8]. Hence, in order to improve overall survival (OS) among patients with HCC, there exists an imperative medical need for development of new therapeutic agents as well as optimal multidrug combination strategies. Perhaps ironically, against the backdrop of apparent contradiction between the lengthy process of *de novo* drug synthesis and urgent requirement of HCC patients, it is necessary for us to find an alternative way of drug management, with a particular focus on drug repurposing.

As mentioned earlier, dogs as the idealized and anthropomorphic model sharing crucial features with humans including similar responses to the same agent, potentially represent a significantly broader population of cancer patients who can be included in the preclinical drug-development path [3]. For instance, two reagents and even their analogs tailored to target canine cancers (*i.e.*, a nonspecific COX inhibitor piroxicam and selective inhibitor of nuclear export (SINE) KPT-330) have already been applied to

suppress the growth of lymphoma and urothelial carcinoma in humans, respectively [9]. Implicit in this paradigm is the hypothesis that there may appear to exist more canine drugs harboring a potential, translational significance to treat a certain form of human tumors. HCC is also prevalent in canines and such canine HCCs share plenty of similarities with human HCC in clinical characteristics and histopathological traits, raising the possibility of agents for canine HCC as a neglected arsenal that can be used for that of humans [10]. Among the authorized drugs used in dogs, toceranib (TOC), an aforementioned RTK inhibitor preliminary proved to be effective for dogs with hepatocellular carcinoma, emerged as a potent candidate pending further experimental investigation [11]. In this regard, another closely related small-molecule inhibitor sunitinib has received FDA approval for treating advanced renal-cell carcinoma in clinic, providing evidence for the feasibility and significance of exploring the effects of TOC on patients suffering from cancer, particularly the human HCC [12].

Herein, we demonstrate that TOC, the first FDA-approved drug for canine cancer, exhibits a potent therapeutic response against human HCC by employing different *in vitro* and *in vivo* models, which occurs as a direct consequence of TOC-triggered apoptosis. Further research indicates that TOC stimulates the expression of cysteine-rich angiogenic inducer 61 (CCN1/Cyr61), a multifunctional extracellular matrix (ECM) protein, which sequentially initiates protective autophagy via its suppression on the Akt/mTOR pathway. Blocking TOC-mediated autophagy reinforces the anti-HCC activity of TOC. Furthermore, TOC enhances the therapeutic response of HCC cells to sorafenib *in vitro* and *in vivo*. Collectively, our findings support a therapeutic role played by TOC against human HCC, as a monotherapy agent or a combination partner with autophagy inhibitors.

2. Materials And Methods

2.1 Cell culture

Human hepatocellular carcinoma cell lines (Huh7, Hep3B, MHCC-97H, PLC/PRF/5 and SK-Hep1) and non-tumor human hepatic cell line (LO2) were all purchased from ATCC. Cells were maintained in DMEM supplemented with 1% streptomycin-penicillin (Sigma) and 10% serum (Biowest) at 37 ℃ in a humidified atmosphere with 5% CO_2.

2.2 Reagents

TOC, CQ (Chloroquine), CHX (Cycloheximide) and MG-132 were purchased from Selleck Chemicals. 3-methyladenine (3-MA) and Z-VAD (Z-Val-Ala-Asp (OMe)-FMK) were purchased from MedChem Express. Lipofectamine 3000 reagent was purchased from Invitrogen. The antibodies involved in this study were listed as following: cleaved caspase-3 (9664S; Cell Signaling Technology, Danvers, MA, USA), PARP (ab74290; Abcam, Cambridge, MA, USA), cleaved PARP (ab32064; Abcam), LC3 (NB100-2220; Novus, Saint Charles, MO, USA), ATG5 (12994S; Cell Signaling Technology), Akt (4685; Cell Signaling Technology), phosphorylated (p-)Akt (Ser473) (4060; Cell Signaling Technology), mTOR (2972; Cell Signaling Technology), p-mTOR (Ser2448) (2971; Cell Signaling Technology), p70S6K (9202; Cell

Signaling Technology), p-p70S6K (Ser371) (9208; Cell Signaling Technology), Cyr61 (122190, ZEN BIO), Ki67 (ab66155; Abcam), β-actin (sc-1616; Santa Cruz Biotechnology), and horseradish peroxidase-conjugated anti-rabbit secondary antibody (sc-2004; Santa Cruz Biotechnology), horseradish peroxidase-conjugated anti-mouse secondary antibody (sc-2005; Santa Cruz Biotechnology).

2.3 Measurement of cell viability

TOC-effects on tumor cell growth were evaluated by MTT (3-(4,5-dimethylthiazol-2-yl)-2,5-diphenylte-trazolium bromide, Sigma) assay and colony formation assay described as before [13], respectively, for short-term and long-term. Cell proliferation was detected emloying the EdU incorporation assay kit (RiboBio Co., Ltd, C10310). And the operation was completely conducted according to the instruction. Images were collected with a fluorescence microscope.

2.4 Lactate dehydrogenase release assay

Cell cytotoxicity of TOC was assessed by lactate dehydrogenase release (LDH) assay, using an LDH test kit (Beyotime Biotechnology, Nanjing, China). The experiment was carried out in accordance with the supplier's instructions.

2.5 Flow cytometry

Cells were harvested after 24 hours TOC treatment, and washed once with PBS, then fixed with 70% medicinal alcohol for 48 hours. These fixed cells prepared for cell cycle analysis (Beyotime Biotechnology, Nanjing, China) were washed with PBS, followed by FACS detection. FlowJo software was applied to data analysis.

2.6 TUNEL assay

Cells were seeded onto glass coverslips in 24-well plates beforehand, subsequently dealing with TOC for 24 hours. 30 mins fixed in 4% paraformaldehyde later, terminal deoxynucleotidyl transferase-mediated nick-end labeling (TUNEL) staining was conducted with the Dead End Fluorometric TUNEL system (Promega). Using a fluorescent microscope, the TUNEL-positive cells were detected and photographed in every independent experiment.

2.7 Transmission electron microscopy

After treated with or without 10 μM TOC, Huh7 and Hep3B cells were fixed in 3% glutaraldehyde. When the samples were embedded after dehydration, ultrathin sections of ~70 nm were prepared and then double stained with 2% uranyl acetate and Reynolds lead citrate. Autophagic vesicles were analyzed by Hitachi HT7800 electron microscopy at 80kV.

2.8 Acridine orange staining

Acridine orange staining assay was performed to evaluate autophagy as described previously [14]. Cells suspended in PBS were stained with 1 mmol/L acridine orange (Sigma-Aldrich) for 5 minutes.

2.9 Immunofluorescence

Cells were plated in glass coverslips in 24-well plates, fixed in 4% formaldehyde for 2 hours, then permeabilized with PBS containing 0.3% Triton X-100 and 5% BSA for 1.5 hours. After that, these cells were incubated with antibodies against LC3 and LAMP2 at 4℃ overnight, and subsequently incubated with Alexa Fluor secondary antibodies for 1.5 hours. Nuclei were stained with DAPI (Santa Cruz Biotechnology). Image capture was performed using confocal laser scanning microscopy (Zeiss).

2.10 RNA interference

The RNA interference assay was conducted using ATG5, Cyr61, and scramble small interfering RNA (siRNA) synthesized by GenePharma (Shanghai, China) following the manufacturer's instructions, using Lipofectamine 3000 reagent (Thermo Fisher Scientific). The sequences of siRNA included in transfection were human *ATG5* siRNA, 5'-GCAACU-CUGGAUGGGAUUGTT-3'; human *Cyr61* siRNA, 5'-AACAUC-AGUGCACAUGUAUUG-3'.

2.11 Western blotting

Cells were harvested after treatment and then lysed in RIPA buffer added with protease and phosphatase inhibitor cocktail (Sigma, p8340). Proteins were isolated using SDS-PAGE and then transferred to a 0.22 μm polyvinylidene difluoride (PVDF) membrane. Blocked the transferred membrane in 5% skimmed milk for 1 hour, and the samples were incubated in suitable primary antibody in 4°C overnight and then incubated with the secondary antibody at room temperature for 1.5 hours. Immunoreactive bands were detected with enhanced chemiluminescence reagent, with β-actin serving as internal control.

2.12 Cellular thermal shift assay

Cells were harvested after treated with or without TOC for 12h and resuspend with PBS. The suspension was divided into six tubes, then heated for 5mins to 54, 57, 60, 64, 67, 70℃ followed by 3 cycles of freeze-thawing with liquid nitrogen and centrifugation at 15000g for 15 mins.

2.13 Animal models

8-week-old male NOD/SCID mice purchased from HFK Bioscience Co., Ltd (Beijing) were employed to establish the orthotopic liver cancer models. Huh7 cells (1×10^6 cells/mouse) were collected and suspended in PBS and engrafted in the mammary fat pad of NOD/SCID mice. Tumor volumes were assessed daily according to the following formula: tumor volume (mm^3) = (length × $width^2$)/2. Mice were randomized into four groups, 0.1 mL of vehicle (physiologic saline), TOC 5 mg/kg, CQ 25 mg/kg, or TOC 5 mg + CQ 25 mg/kg, when the tumor volumes reached ~100 mm^3. Mice in all groups were administered orally once a day. When significant differences were obtained between the four groups, they were euthanized for analysis. All procedures performed on mice in our study were approved by the Institutional Animal Care and Treatment Committee of Sichuan University.

2.14 Immunohistochemistry

The tumor samples and major organs from xenograft models were embedded in paraffin and cut into 4-μm-thick sections. All sections were dewaxed, rehydrated, then quenched the endogenous peroxidase activity, then treated with citrate buffer to remove antigen. After incubation with indicated primary antibodies at 4°C overnight, sections were stained with diaminobenzidine and re-stained with Mayer hematoxylin. H&E staining was done to the major organs (heart, liver, spleen, lung, and kidney) sections. Imaging was visualized with DM2500 fluorescence microscope.

2.15 Statistical analysis

Statistical analysis was done using GraphPad Prism 8. Statistical differences were calculated using one-way ANOVA or Student's t test. Herein, two-tailed P values of less than 0.05 were considered statistically significant. Unless otherwise stated, data were described as mean ± SEM.

3. Results

3.1 TOC exhibits potent anti-HCC effects by inducing apoptosis *in vitro* and *in vivo*

The chemical structure of TOC, a chemotherapeutic agent for canine carcinoma, is shown in Fig. 1A. To define the antitumor effects of TOC on human HCC *in vivo*, we undertook to perform an MTT assay using five different human HCC cell lines (Huh7, Hep3B, MHCC-97H, PLC/PRF/5 and SK-Hep1) and a non-tumorigenic human hepatocyte cell line (LO2). As expected, the cell viability of HCC cell lines (IC_{50} values ranging from 5.90 to 12.35 μM) was repressed greater than that of LO2 cell line following TOC exposure in a dose- and time-dependent manner (Fig. 1B and Fig S1A). Because this repression was most significant in Huh7 and Hep3B cells, these two types of HCC cell lines were chosen as representatives for the follow-up exploration. Consistently, TOC treatment also resulted in a lower clonogenic capability of HCC cells compared to that of LO2 cells through 2D (plate)-colony formation assay (Fig. 1C). In addition to this tumor-specific growth inhibitory effect exerted by TOC, the reduced proliferative potential as well as enhanced cytotoxicity were further observed in HCC cells via EdU incorporation and lactate dehydrogenase (LDH) assays (Fig. 1D-E and Fig. S1B). Next, it was demonstrated that this impaired proliferative capacity was largely due to TOC-induced cell-cycle arrest in a dose-dependent manner, manifested by a gradually increasing percentage of G0/G1 arrested HCC cells (Fig. S1C). As for the effective cytotoxicity of TOC against HCC cells, we were curious if its killing effect on Huh7 and Hep3B cells was associated with apoptotic cell death, given the fact that apoptosis is the most common way by which an antineoplastic agent works. As predicted, we observed that TOC-treated cells have undergone significant morphological changes, which were manifested by the formation of intracytoplasmic vacuoles and signs of apoptosis (Fig. 1F). The expression levels of apoptotic markers, *i.e.*, cleaved caspase 3 and cleaved PARP, were simultaneously upregulated in HCC cells as the increment of TOC dose

(Fig. 1G), indicating an apoptosis-promoting role played by TOC, as was the case displayed in TUNEL assay (Fig. S1D). Moreover, incubating HCC cells with apoptosis inhibitor Z-VAD-FMK and TOC could partially alleviate the growth-inhibitory effect of TOC that was reflected on improved cell viability when compared to the group without Z-VAD-FMK treatment (Fig. 1H). To summarize, these results indicated that TOC exhibits potent anti-HCC effects *in vitro* via activating apoptosis.

To extend and generalize these findings further, we developed an HCC cell-line (Huh7) derived xenograft mouse model to evaluate the therapeutic effect of TOC against HCC *in vivo*. Consistently, in comparison with animals in the vehicle group, mice administered with TOC showed a dramatic reduction of tumor size and weight (Fig. 1I-K). Corresponding to that, the TOC-treated group compared with vehicle-treated ones exhibited a lower level of Ki67 (a reliable indicator of proliferation) and an increased expression of cleaved caspase 3 in xenograft tumors by immunohistochemical (IHC) staining (Fig. 1L-M). Collectively, these results demonstrated that TOC inhibits HCC cell growth both *in vitro* and *in vivo* through TOC-mediated apoptosis.

3.2 TOC elicits autophagy in HCC cells

An increasing number of studies have indicated the importance of drug-induced autophagy in cancer therapy [15,16]. It has been reported that sunitinib, a multityrosine kinase inhibitor sharing structural and functional similarity with TOC, served a controversial role in autophagy regulation within multiple cancers [17], which raised the question of whether TOC can also act as an autophagy regulator in HCC cells. Immunoblotting analysis of autophagy markers were performed to investigate whether TOC modulates autophagy in HCC cells, which revealed that Huh7 and Hep3B cells exhibited dramatic autophagic induction in a dose- and time-dependent manner upon TOC treatment, as demonstrated by enhanced expression of LC3-II, ATG5 and p62 (Fig. 2A-B). Furthermore, as evidenced by transmission electron microscopy and immunofluorescence analyses, there was a significant accumulation of autophagic vesicles and LC3 puncta in Huh7 and Hep3B cells after TOC-treatment (Fig. 2C-D). Consistently, xenograft tumors exhibited increased expression of LC3B following TOC administration (Fig. 2E). Notably, this induction manifested by TOC-triggered accumulation of LC3-II, could be intensively attenuated by pharmacological inhibition of autophagy initiation employing 3-methyladenine (3-MA) (an inhibitor of class III PI3K), or through genetic silencing of *ATG5* (a key inducer of autophagosome formation) in HCC cells (Fig. 2F-H and Fig. S2A). The TOC-induced autophagy in HCC was further verified by the observation that TOC treatment resulted in increased interaction of Beclin1 with Atg14L and the dissociation of Beclin1 with Bcl-2 (Fig. S2B), which is an important initial event in autophagy. Wherever, we didn't observe the phenomenon of autophagy in LO2 cell treated with TOC (Fig. S2C-D). Altogether, these data suggested the stimulative effects of TOC on autophagy initiation in HCC cells.

3.3 TOC promotes autophagy flux in HCC cells

Considering that TOC-mediated LC3-II accumulation may be attributed to autophagy initiation or impaired autophagy flux, we next evaluated the autophagy flux upon TOC treatment. As depicted in Fig. 3A, the combinatorial treatment of TOC with chloroquine (CQ) (a late-autophagy inhibitor) led to a substantial

accumulation of LC3-II compared to a single treatment of TOC or CQ, implying that TOC may prompt autophagic flux in HCC cells. This notion was further validated by the observation indicating significant colocalization of LC3B and LAMP2 in HCC cells treated with TOC rather than CQ, a symbol of the fusion of autophagosomes and lysosomes (Fig. 3B), which concerted with the results from lysotracker red-staining (Fig. S3A). Consistently, using tandem mRFP-GFP-LC3 constructs, there emerged increased autolysosomes (red dots, RFP^+ GFP^-) accompanied by reduced autophagosomes (yellow dots, RFP^+ GFP^+) in TOC-treated HCC cells in contrast to that detected in CQ-treated cells (Fig. 3C). Moreover, in response to TOC treatment, the induced formation of autophagic vacuoles was monitored by acridine orange (AO) staining (Fig. 3D). In summary, these results indicated that TOC boosts autophagic flux in HCC cells.

3.4 Inhibition of autophagy enhances the anti-HCC effects of TOC

It is firmly believed that the role of autophagy is context-dependent, which could be cytoprotective, cytostatic or cytotoxic to tumor cells [18]. Curious about the function of TOC-activated autophagy in HCC, we thus assessed the impacts of TOC on HCC growth in combination with a series of inhibitors targeting different autophagic phases. Strikingly, the anti-HCC efficacy of TOC could be significantly exacerbated through both inhibition of initial-stage and late-stage autophagy (3-MA and CQ, respectively), or by genetic silencing of *ATG5*, evidenced by a drastic reduction in cell viability, clonogenic capacity and proliferative potential compared with that of group treated with TOC alone (Fig. 4A-D and Fig. S4A-E). This pro-survival role of TOC-induced autophagy *in vitro* was further verified by *in vivo* studies, reflected by the greatly decreased tumor size, growth rate, and weight without obvious weight loss and visceral toxicity following TOC/CQ combination therapy compared to either treatment alone (Fig. 4E-G and Fig. S4F-G). Consistently, the Ki67 level was much lower in the combinatorial treated tissues detected by IHC staining (Fig. 4H). Overall, these data highlighted that TOC-triggered autophagy might show a cytoprotective effect on HCC, elucidating that anti-HCC potency caused by TOC could be further strengthened when combined with autophagy inhibitors such as CQ.

3.5 TOC induces autophagy by repressing the Akt/mTOR pathway in HCC cells

Cumulative evidence has supported Akt/mTOR signaling pathway as a major regulator of autophagy [19]. Therefore, we assumed that Akt/mTOR pathway might be responsible for TOC-induced autophagy. In line with our speculation, TOC in a dose- and time-dependent manner decreased the expression of phosphorylated- (p-)Akt, mTOR, and p70S6K in HCC cells (Fig. 5A-B), accompanied by the decreased expression of p-Akt in xenograft tumors from TOC-treated mice (Fig. 5C). Along this line, we then transfected HCC cells with CA-Akt (a constitutively active form of Akt) and found that TOC-mediated autophagy was markedly counteracted by CA-Akt, manifested by a decreased number of LC3 puncta and downregulation of LC3-II (Fig. 5D-E). These events could well prove the involvement of Akt/mTOR signaling in TOC-triggered autophagy. Echoing the effects of autophagy inhibition, it was demonstrated

using MTT and colony formation assay that TOC-induced growth suppression, manifested by decreased cell viability and lower clonogenic ability, was potentiated in Huh7 and Hep3B cells transfected with CA-Akt (Fig. 5F, G). Taken together, these results implied that autophagy activation is driven by TOC-mediated impaired Akt/mTOR pathway in HCC cells.

3.6 TOC facilitates autophagy through Cyr61/Akt axis in HCC cells

There have been considerable reports about the contribution made by Cyr61 (a secreted matricellular protein) to Akt inactivation [20]. To explore whether Cyr61 was involved in TOC-induced Akt inactivation, we conducted western blot analysis of Cyr61, which revealed the upregulation of Cyr61 in Huh7 and Hep3B cells exposed to TOC (Fig. 6A). Similar observations were generated by *in vivo* models (Fig. 6B). Furthermore, the treatment of TOC could engage and stabilize Cyr61 against thermal changes in the cellular thermal shift assay (Fig. 6C), and the rate of CYR61-degration was enhanced by MG-132 (Fig. S5A). In addition to this preliminary finding of a correlation between TOC treatment and upregulation of Cyr61, we were curious to determine whether Cyr61 was required for TOC-induced Akt suppression and further autophagy induction. As expected, TOC-induced Akt inactivation, LC3-II conversion, and LC3 puncta accumulation were all weakened by genetic silencing of *Cyr61* (Fig. 6D-E); in contrast, exogenous Cyr61 expression resulted in elevated conversion of LC3-I to LC3-II (Fig. S5B), LC3 puncta formation (Fig. S5C), and decreased p-Akt level (Fig. 6F), similar to that observed in cells treated with TOC alone. Beyond that, the Cyr61-mediated enhancement of LC3 puncta accumulation and LC3 lipidation was found to be counteracted through CA-Akt, further confirming the involvement of Cyr61 in inactivated Akt-stimulated autophagy in TOC-treated HCC cells (Fig. 6F and Fig. S5D). Given that TOC could induce growth inhibition in HCC cells, we then addressed whether Cyr61 functioned in this process. Intriguingly, the inhibitory effects of TOC on HCC growth could be markedly obstructed by genetic inhibition of *Cyr61*, as evidenced by the results from MTT and colony formation assay (Fig. 6G and Fig. S5E). In accordance with this finding hinting a tumor-suppressive role of Cyr61 in HCC, a low expression level of Cyr61 in clinical tissues was confirmed by Oncomine datasets (Fig. 6H). To further investigate the prognostic value of Cyr61 in HCC, the correlation of Cyr61 expression with patient survival was evaluated by applying the TCGA database, which illustrated that high level of Cyr61 was correlated with favorable survival outcomes (Fig. 6I). In conclusion, TOC inactivates Akt/mTOR signaling pathway and thereby elicits autophagy with the engagement of Cyr61.

3.7 TOC acts as a combinatorial partner of sorafenib

Sorafenib (SOR), a first-line chemotherapeutic agent remaining the only approved systemic therapy for advanced HCC patients, possesses antiproliferative, antiangiogenic, and proapoptotic properties [8]. Despite its capacity to extend overall survival, in actual fact, this clinical benefit is quite limited due to the early occurrence of resistance in most cases [21,22]. Thus, combining standard therapy (sorafenib treatment) with other novel drugs effective for HCC might be a rational and promising approach to overcoming sorafenib resistance. In this regard, we evaluated the impacts of TOC on the response of HCC

cells to sorafenib treatment *in vitro*. As shown in Fig. 7A, the HCC cell growth was repressed by SOR with IC_{50} values ranging from 10 to 20 μM in Huh7 and Hep3B cells, while the combinatorial treatment of TOC and SOR showed an additive effect which was reflected on strongly decreased cell viability and impaired clonogenic capability in contrast to the group with single treatment of TOC or SOR (Fig. 7B-C). The synergistic effects of TOC and SOR were further confirmed *in vivo* by the Huh7 xenograft model, as demonstrated by a slower tumor growth rate and remarkably reduced tumor size and weight in the combinatorial treated group (Fig. 7D-F). Furthermore, xenograft tumors with combinatorial treatment exhibited decreased expression of ki67 in comparison with TOC or sorafenib-treated ones (Fig. 7G). Taken together, these analyses indicated the potential of TOC application in both single-modality treatment and combined pharmacotherapy for HCC.

4. Discussion

Drug repurposing, known as identifying new indications for approved drugs, offers a shorter approval process for cancer therapy [23,24]. Several studies have proved that drug repurposing from canine drugs may reveal new targets and pathways for human HCC [16,25], particularly the small molecule kinase inhibitors [26,27]. TOC, an orally bioavailable multi-targeted inhibitor blocking receptor tyrosine kinase (RTK), is generally active against several split kinase families, including VEGFR, PDGFR, Kit, and Ret [28]. For its inhibition of VEGFR and PDGFR known to function in tumor-driven angiogenesis, TOC was initially developed as an antiangiogenic drug, displaying a biological activity in various cancer models [4]. In addition to its impacts on angiogenesis, TOC might also directly inhibit tumor growth via targeting Kit and Ret [29]. Similar to TOC in terms of structure and function, another RTK inhibitor sunitinib (Sutent) which shares the same targets with TOC, has been reported to exert single-agent activity in HCC, hinting at a potential role of TOC in HCC therapy [30]. Our present study demonstrated that TOC has a potent anti-cancer effect in HCC both *in vitro* and *in vivo*, driven mainly by TOC-stimulated apoptosis in HCC cells. In addition to apoptosis induced by TOC, TOC was demonstrated to activate protective autophagy via the Cyr61-Akt/mTOR axis. Considering this pro-survival role, blocking autophagy using autophagic inhibitors could enhance anti-HCC efficacy mediated by TOC. Our findings may extend the clinical potential of TOC and provide a new paradigm for HCC therapy.

In general, autophagy, considered as a survival mechanism that maintains cell homeostasis, is a mechanism by which cellular materials are delivered to lysosomes for a multi-step degradation process [31]. Growing evidence has proven that autophagy may play context-dependent roles in different tumors or the same tumor at different stages. Furthermore, regulating autophagy has been recognized as a promising therapeutic strategy [32,33]. Apoptosis, an autonomic regulated physiological process also known as type I programmed cell death (PCD I) characterized by cell membrane blebbing and chromosomal DNA fragmentation [34], has long been considered a popular target in different cancer treatment strategies [35]. Both autophagy and apoptosis are typically programmed cell death regulated by

complicated signal transduction networks, and thus their dysregulation may ultimately contribute to tumor development. Recent studies suggest complex interactions between autophagy and apoptosis with contexts of both physiological and pathological, which have been widely studied mainly for their significance in cancer therapy [36]. In this regard, autophagy usually occurs in advance of apoptosis within the same cell. Meanwhile, whether autophagy activates or suppresses apoptosis depends on specific cell types, stress, or stimuli [37]. In addition to the regulatory role of autophagy in the apoptosis process, there are indeed reports stating that several proteins known to modulate apoptosis might act as inducers of autophagy as well [38]. In this study, we demonstrated that TOC inhibited the growth of HCC cells *in vitro* and *in vivo* with the enhancement of both autophagy and apoptosis in response to TOC. However, the connection between them remained uncharacterized in this study. Notably, increasing evidence has proved the close correlation between autophagy mechanism and drug resistance [39]. In this context, there are quite a few cases that some compounds have been used to treat cancers (such as frontline glioma [40], colon cancer [41], pancreas cancer [42]) in conjunction with autophagy inhibitor CQ/HCQ in clinical trials. In this regard, TOC-induced autophagy played a cell-protective role in treating HCC, suggesting that the combination of autophagy inhibitors with TOC may provide better cancer treatment. However, given the issue above that autophagy likely affects apoptosis in the opposing directions, the underlying problem of autophagy manipulation is highlighted in clinical practice; that is, blocking autophagy may show no influence on the improvement of response to partner agents, partially owing to the degradation of different pro- or anti-apoptotic regulators by autophagy [43]. The principles behind such combination treatments largely remain unknown as most combinations were introduced based on experimentation among patients. Therefore, the real issue is to evaluate and determine which member possesses a more significant weight in monitoring cellular fate [44].

The Akt/mTOR signaling pathway is well-recognized in autophagy and apoptosis. Hence, a series of agents targeting the Akt/mTOR-mediated autophagy display considerable anti-tumor effects and promising clinical application prospects in malignancies [19,45]. Following this, we found TOC decreased phosphorylation levels of Akt and mTOR, which were crucial for the initiation of autophagy in TOC-treated HCC cells. Furthermore, the upstream of mTOR, PI3K/Akt pathway could be inhibited by a secreted matricellular protein Cyr61 (cysteine-rich 61/CCN1), a member of the CCN protein family. Past studies have shown that the function of Cyr61 depends on the complex cellular context [31]. Here, we found that Cyr61 was expressed at a low level in HCC cell lines, in accordance with previous reports [34]. Further investigation showed that elevated Cyr61 could inactivate Akt upon TOC exposure, thus giving rise to the initiation of protective autophagy conferring resistance to TOC in HCC cells. Thus, we proposed a novel mechanism of Cyr61/Akt axis in the context of TOC treatment.

5. Conclusion

In conclusion, our results have demonstrated that the canine drug TOC could be a promising anti-cancer drug for the treatment of human HCC via inducing apoptosis. Intriguingly, TOC could activate protective autophagy in HCC cells with the involvement of Cyr61/Akt axis, and therefore combined use of TOC and

autophagy inhibitors could further strengthen its anti-HCC activity. Enlightened by such a mode of action, there is reason to believe that repurposing canine drugs for human use is not confined to TOC for HCC, but can be extended to other canine drugs for a broad spectrum of human malignancies, and therefore further investigation is merited.

Abbreviations

3-MA
3-methyladenine
AO
acridine orange
CQ/HCQ
chloroquine/ hydroxychloroquine
Cyr61
cysteine-rich 61/CCN1
ECM
extracellular matrix
FDA
Food and Drug Administration
HCC
Human hepatocellular carcinoma
IHC immunohistochemical
LDH
lactate dehydrogenase release assay
MTT
3-(4,5-dimethylthiazol-2-yl)-2,5-diphenylte-trazolium bromide
OS
overall survival
RKT
receptor tyrosine kinase
SOR
sorafenib
TKI
tyrosine kinase inhibitors
TOC
toceranib phosphate.

Declarations

Acknowledgements

Not applicable.

Authors' Contributions

C.H. designed and supervised the research. L.Q., N.W., Z.Z., M.L. and B.L. performed the experiments. S.Q., M.L. and B.L. performed bioinformatic analysis. L.Q., S.Q. and N.W. developed the animal models. C.H. and S.Q. wrote the manuscript.

Funding

This work was supported by Guangdong Basic and Applied Basic Research Foundation (2019B030302012), National Key Research and Development Project of China (2020YFA0509400, 2020YFC2002705), Chinese NSFC (81821002, 81790251, 82130082).

Availability of data and material

Not applicable.

Consent for publication

Not applicable.

Competing interests

The authors declare no potential conflicts of interest.

Ethics approval and consent to participate

Not applicable.

References

1. LeBlanc, A. K. & Mazcko, C. N. Improving human cancer therapy through the evaluation of pet dogs. *Nat Rev Cancer* **20**, 727-742, doi:10.1038/s41568-020-0297-3 (2020).
2. Gustafson, D. L., Duval, D. L., Regan, D. P. & Thamm, D. H. Canine sarcomas as a surrogate for the human disease. *Pharmacol Ther* **188**, 80-96, doi:10.1016/j.pharmthera.2018.01.012 (2018).
3. Gardner, H. L., Fenger, J. M. & London, C. A. Dogs as a Model for Cancer. *Annu Rev Anim Biosci* **4**, 199-222, doi:10.1146/annurev-animal-022114-110911 (2016).
4. Mendel, D. B. *et al.* In vivo antitumor activity of SU11248, a novel tyrosine kinase inhibitor targeting vascular endothelial growth factor and platelet-derived growth factor receptors: determination of a pharmacokinetic/pharmacodynamic relationship. *Clin Cancer Res* **9**, 327-337 (2003).
5. Greten, T. F., Lai, C. W., Li, G. & Staveley-O'Carroll, K. F. Targeted and Immune-Based Therapies for Hepatocellular Carcinoma. *Gastroenterology* **156**, 510-524, doi:10.1053/j.gastro.2018.09.051 (2019).

6. Forner, A., Reig, M. & Bruix, J. Hepatocellular carcinoma. *Lancet* **391**, 1301-1314, doi:10.1016/S0140-6736(18)30010-2 (2018).
7. Llovet, J. M., Montal, R., Sia, D. & Finn, R. S. Molecular therapies and precision medicine for hepatocellular carcinoma. *Nat Rev Clin Oncol* **15**, 599-616, doi:10.1038/s41571-018-0073-4 (2018).
8. Xia, S., Pan, Y., Liang, Y., Xu, J. & Cai, X. The microenvironmental and metabolic aspects of sorafenib resistance in hepatocellular carcinoma. *EBioMedicine* **51**, 102610, doi:10.1016/j.ebiom.2019.102610 (2020).
9. Lucroy, M. D. & Suckow, M. A. Predictive modeling for cancer drug discovery using canine models. *Expert Opin Drug Discov* **15**, 731-738, doi:10.1080/17460441.2020.1739644 (2020).
10. Partridge, B. R. *et al.* High-Frequency Irreversible Electroporation for Treatment of Primary Liver Cancer: A Proof-of-Principle Study in Canine Hepatocellular Carcinoma. *J Vasc Interv Radiol* **31**, 482-491 e484, doi:10.1016/j.jvir.2019.10.015 (2020).
11. Heishima, K. *et al.* Short-Term Administration of Single-Agent Toceranib in Six Cases of Inoperable Massive Canine Hepatocellular Carcinoma. *J Am Anim Hosp Assoc*, doi:10.5326/JAAHA-MS-6788 (2018).
12. Motzer, R. J. *et al.* Sunitinib versus interferon alfa in metastatic renal-cell carcinoma. *N Engl J Med* **356**, 115-124, doi:10.1056/NEJMoa065044 (2007).
13. Dou, Q. *et al.* Ivermectin Induces Cytostatic Autophagy by Blocking the PAK1/Akt Axis in Breast Cancer. *Cancer Res* **76**, 4457-4469, doi:10.1158/0008-5472.CAN-15-2887 (2016).
14. Wang, K. *et al.* Quercetin induces protective autophagy in gastric cancer cells: involvement of Akt-mTOR- and hypoxia-induced factor 1alpha-mediated signaling. *Autophagy* **7**, 966-978, doi:10.4161/auto.7.9.15863 (2011).
15. Levy, J. M. M., Towers, C. G. & Thorburn, A. Targeting autophagy in cancer. *Nat Rev Cancer* **17**, 528-542, doi:10.1038/nrc.2017.53 (2017).
16. Zhong, Z., Sanchez-Lopez, E. & Karin, M. Autophagy, Inflammation, and Immunity: A Troika Governing Cancer and Its Treatment. *Cell* **166**, 288-298, doi:10.1016/j.cell.2016.05.051 (2016).
17. Abdel-Aziz, A. K., Abdel-Naim, A. B., Shouman, S., Minucci, S. & Elgendy, M. From Resistance to Sensitivity: Insights and Implications of Biphasic Modulation of Autophagy by Sunitinib. *Front Pharmacol* **8**, 718, doi:10.3389/fphar.2017.00718 (2017).
18. Dikic, I. & Elazar, Z. Mechanism and medical implications of mammalian autophagy. *Nat Rev Mol Cell Biol* **19**, 349-364, doi:10.1038/s41580-018-0003-4 (2018).
19. Liu, G. Y. & Sabatini, D. M. mTOR at the nexus of nutrition, growth, ageing and disease. *Nat Rev Mol Cell Biol* **21**, 183-203, doi:10.1038/s41580-019-0199-y (2020).
20. Lee, Y. J., Lee, D. M. & Lee, S. H. Production of Cyr61 protein is modulated by extracellular acidification and PI3K/Akt signaling in prostate carcinoma PC-3 cells. *Food Chem Toxicol* **58**, 169-176, doi:10.1016/j.fct.2013.04.035 (2013).

21. Sun, X. *et al.* Metallothionein-1G facilitates sorafenib resistance through inhibition of ferroptosis. *Hepatology* **64**, 488-500, doi:10.1002/hep.28574 (2016).
22. Mendez-Blanco, C., Fondevila, F., Garcia-Palomo, A., Gonzalez-Gallego, J. & Mauriz, J. L. Sorafenib resistance in hepatocarcinoma: role of hypoxia-inducible factors. *Exp Mol Med* **50**, 1-9, doi:10.1038/s12276-018-0159-1 (2018).
23. Pushpakom, S. *et al.* Drug repurposing: progress, challenges and recommendations. *Nat Rev Drug Discov* **18**, 41-58, doi:10.1038/nrd.2018.168 (2019).
24. Wu, P. *et al.* Adaptive Mechanisms of Tumor Therapy Resistance Driven by Tumor Microenvironment. *Front Cell Dev Biol* **9**, 641469, doi:10.3389/fcell.2021.641469 (2021).
25. Fulda, S. Targeting autophagy for the treatment of cancer. *Biol Chem* **399**, 673-677, doi:10.1515/hsz-2018-0105 (2018).
26. Carter, T. A. *et al.* Inhibition of drug-resistant mutants of ABL, KIT, and EGF receptor kinases. *Proc Natl Acad Sci U S A* **102**, 11011-11016, doi:10.1073/pnas.0504952102 (2005).
27. Hsieh, Y. Y., Chou, C. J., Lo, H. L. & Yang, P. M. Repositioning of a cyclin-dependent kinase inhibitor GW8510 as a ribonucleotide reductase M2 inhibitor to treat human colorectal cancer. *Cell Death Discov* **2**, 16027, doi:10.1038/cddiscovery.2016.27 (2016).
28. London, C. A. *et al.* Phase I dose-escalating study of SU11654, a small molecule receptor tyrosine kinase inhibitor, in dogs with spontaneous malignancies. *Clin Cancer Res* **9**, 2755-2768 (2003).
29. Gan, H. K., Seruga, B. & Knox, J. J. Sunitinib in solid tumors. *Expert Opin Investig Drugs* **18**, 821-834, doi:10.1517/13543780902980171 (2009).
30. Chow, L. Q. & Eckhardt, S. G. Sunitinib: from rational design to clinical efficacy. *J Clin Oncol* **25**, 884-896, doi:10.1200/JCO.2006.06.3602 (2007).
31. Fernandez, A. F. *et al.* Disruption of the beclin 1-BCL2 autophagy regulatory complex promotes longevity in mice. *Nature* **558**, 136-140, doi:10.1038/s41586-018-0162-7 (2018).
32. Amaravadi, R. K. *et al.* Principles and current strategies for targeting autophagy for cancer treatment. *Clin Cancer Res* **17**, 654-666, doi:10.1158/1078-0432.CCR-10-2634 (2011).
33. White, E., Mehnert, J. M. & Chan, C. S. Autophagy, Metabolism, and Cancer. *Clin Cancer Res* **21**, 5037-5046, doi:10.1158/1078-0432.CCR-15-0490 (2015).
34. Burgess, D. J. Apoptosis: Refined and lethal. *Nat Rev Cancer* **13**, 79, doi:10.1038/nrc3462 (2013).
35. Wong, R. S. Apoptosis in cancer: from pathogenesis to treatment. *J Exp Clin Cancer Res* **30**, 87, doi:10.1186/1756-9966-30-87 (2011).
36. Eisenberg-Lerner, A., Bialik, S., Simon, H. U. & Kimchi, A. Life and death partners: apoptosis, autophagy and the cross-talk between them. *Cell Death Differ* **16**, 966-975, doi:10.1038/cdd.2009.33 (2009).
37. Marino, G., Niso-Santano, M., Baehrecke, E. H. & Kroemer, G. Self-consumption: the interplay of autophagy and apoptosis. *Nat Rev Mol Cell Biol* **15**, 81-94, doi:10.1038/nrm3735 (2014).

38. Mukhopadhyay, S., Panda, P. K., Sinha, N., Das, D. N. & Bhutia, S. K. Autophagy and apoptosis: where do they meet? *Apoptosis* **19**, 555-566, doi:10.1007/s10495-014-0967-2 (2014).
39. Das, C. K., Mandal, M. & Kogel, D. Pro-survival autophagy and cancer cell resistance to therapy. *Cancer Metastasis Rev* **37**, 749-766, doi:10.1007/s10555-018-9727-z (2018).
40. Rosenfeld, M. R. *et al.* A phase I/II trial of hydroxychloroquine in conjunction with radiation therapy and concurrent and adjuvant temozolomide in patients with newly diagnosed glioblastoma multiforme. *Autophagy* **10**, 1359-1368, doi:10.4161/auto.28984 (2014).
41. Patel, S. *et al.* Vorinostat and hydroxychloroquine improve immunity and inhibit autophagy in metastatic colorectal cancer. *Oncotarget* **7**, 59087-59097, doi:10.18632/oncotarget.10824 (2016).
42. Karasic, T. B. *et al.* Effect of Gemcitabine and nab-Paclitaxel With or Without Hydroxychloroquine on Patients With Advanced Pancreatic Cancer: A Phase 2 Randomized Clinical Trial. *JAMA Oncol* **5**, 993-998, doi:10.1001/jamaoncol.2019.0684 (2019).
43. Thorburn, J. *et al.* Autophagy controls the kinetics and extent of mitochondrial apoptosis by regulating PUMA levels. *Cell Rep* **7**, 45-52, doi:10.1016/j.celrep.2014.02.036 (2014).
44. Han, K. *et al.* Synergistic drug combinations for cancer identified in a CRISPR screen for pairwise genetic interactions. *Nat Biotechnol* **35**, 463-474, doi:10.1038/nbt.3834 (2017).
45. Mizushima, N. & Levine, B. Autophagy in Human Diseases. *N Engl J Med* **383**, 1564-1576, doi:10.1056/NEJMra2022774 (2020).

Figures

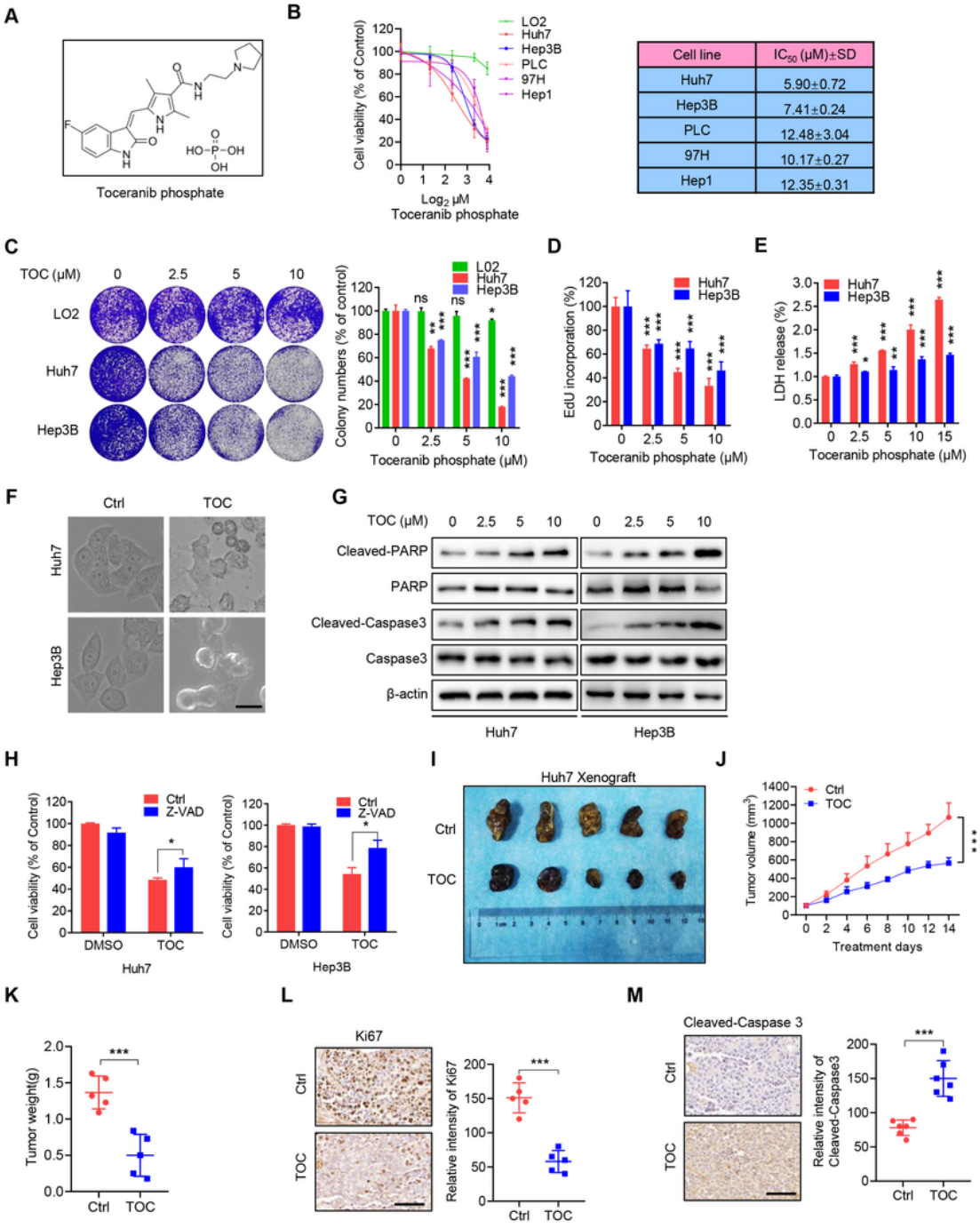

Figure 1

TOC exhibits potent anti-HCC effects by inducing apoptosis *in vitro and in vivo.* (A) The chemical structure of TOC. (B) MTT assay of HCC cell lines and LO2 incubated with indicated concentrations of TOC for 24 h (left). The IC50 value (μM) of cell lines (right). (C, D) HCC cells were treated with indicated concentrations of TOC. Cell proliferation was measured by colony formation assay (C) and EdU incorporation assay (D). (E) LDH release assay of HCC cells subjected to TOC for 24 h. (F) Morphology of

Huh7 and Hep3B cells treated with or without TOC for 24 h. Scale bar, 100 μm. (G) Immunoblotting analysis of total and cleaved PARP or caspase 3 in Huh7 and Hep3B cells treated with indicated concentrations of TOC for 24 h. (H) The MTT assay of Huh7 and Hep3B cells treated with or without TOC (10 μM, 24 h) in the presence or absence of Z-VAD. (I) The images of isolated tumors derived from vehicle or TOC-treated mice bearing Huh7 subcutaneous tumor xenografts. (J, K) The volume and weight in (H). (L, M) Immunohistochemical staining of Ki67 and cleaved-caspase3 in tumor tissues. Scale bar, 50 μm. (*, P <0.05; **, P< 0.01; ***, P < 0.001).

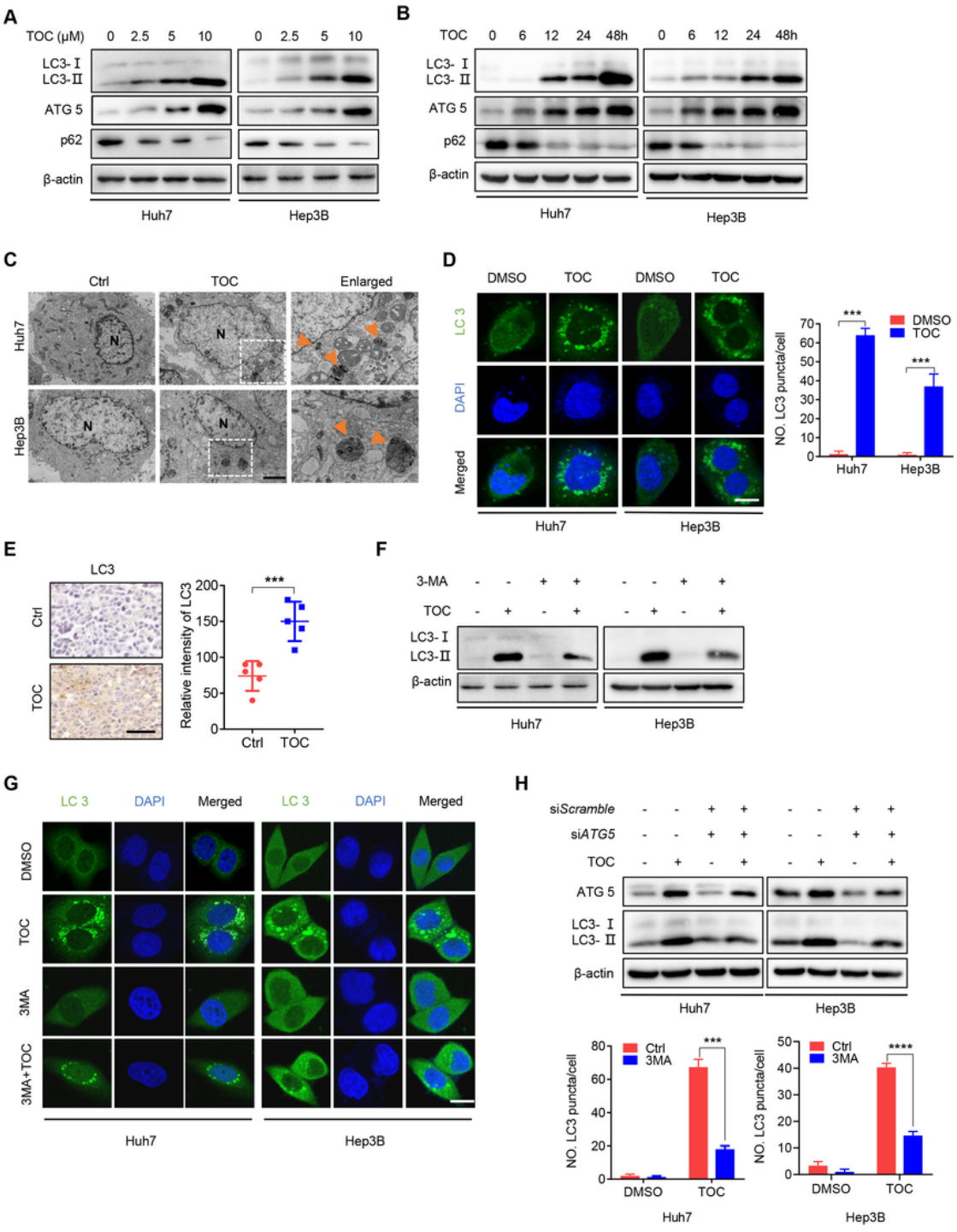

Figure 2

TOC elicits autophagy in HCC cells. (A, B) Immunoblotting analysis of LC3, ATG5, and p62 in Huh7 and Hep3B cells treated with indicated concentrations of TOC for 24 h, or 10 μM TOC for indicated times. (C) Autophagic vesicles were detected by transmission electron microscope in Huh7 and Hep3B cells treated with or without 10 μM TOC for 24 h. Scale bar:2μm. N, nucleus. Arrows, autophagic vesicles. (D) Immunofluorescence analysis of LC3 in HCC cells treated with or without TOC (10 μM, 24 h) (left). The number of LC3 puncta was shown (right). Scale bar, 20 μm. (E) Immunohistochemical staining of LC3 in tumor tissues. Scale bar, 50 μm. (F) Immunoblotting analysis of LC3 in HCC cells treated with or without TOC (10 μM, 24 h) in the presence or absence of 3-MA (10 mM). (G) Immunofluorescence analysis of LC3 in HCC cells treated as in (F). Scale bar, 20μm. (H) Immunoblotting analysis of LC3 in HCC cells transfected with si*Scramble*, si*ATG5* for 24 h, followed by treatment with or without TOC (10 μM, 24 h). Scale bar, 20 μm. (*, P <0.05; **, P< 0.01; ***, P < 0.001).

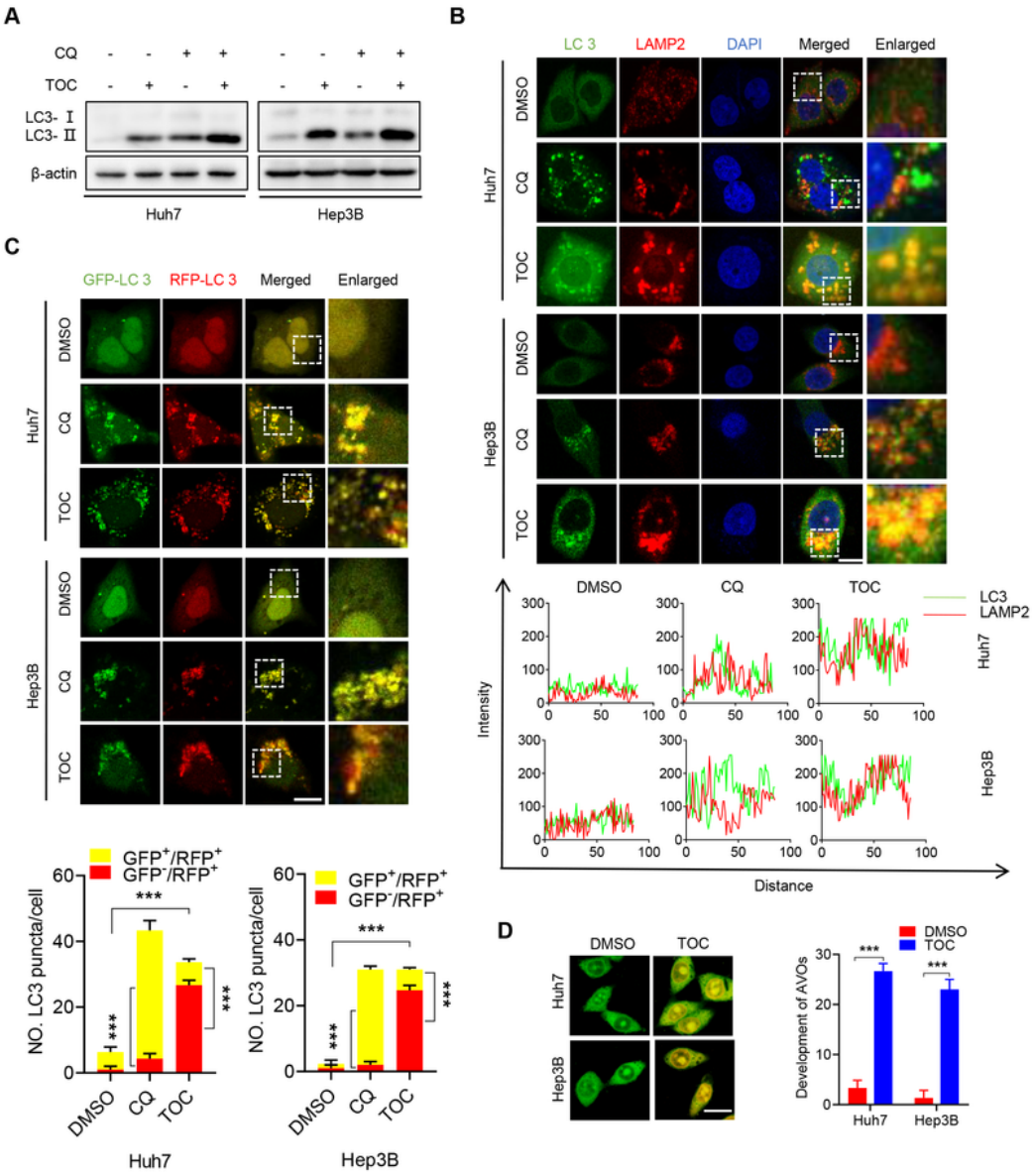

Figure 3

TOC promotes autophagic flux in HCC cells. (A) Immunoblotting analysis of LC3 in Huh7 and Hep3B cells treated with or without TOC (10 μM, 24 h) in the presence or absence of CQ (10 μM). (B) Immunofluorescence analysis of colocalization of LC3 and LAMP2 in HCC cells treated with or without TOC (10 μM, 24 h). (C) Immunofluorescence analysis of HCC cells transfected with RFP-GFP-LC3 and treated with or without TOC (10 μM, 24 h). Cells treated with CQ served as a negative control in (B, C).

Scale bar, 20 μm. (D) Acridine orange staining of HCC cells treated as in (B). Scale bar, 20 μm. (*, P <0.05; **, P< 0.01; ***, P < 0.001).

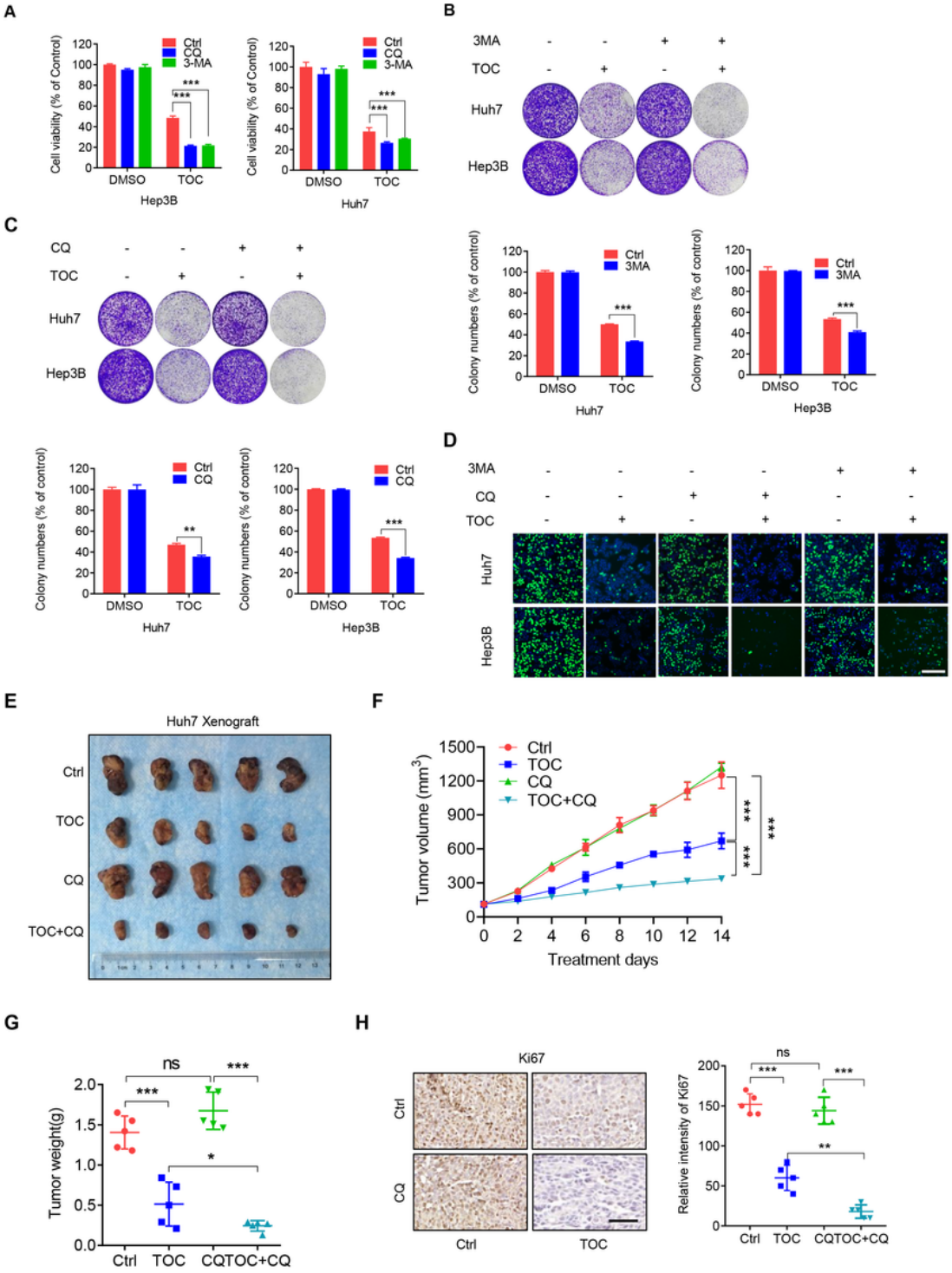

Figure 4

Blockage of autophagy aggravates the TOC-triggered HCC cell death. (A) The MTT assay of Huh7 and Hep3B cells treated with TOC (10 μM, 24 h) in the absence or presence of CQ (10 μM) or 3-MA (10 mM).

(B, C) Colony formation assay of HCC cells treated with TOC (10 μM, 24 h) in the presence or absence of 3-MA (10 mM) or CQ (10 μM). (D) EdU incorporation assay of HCC cells treated as in (A). Scale bar, 50 μm. (E) The images of isolated tumors derived from vehicle or TOC-treated mice with or without CQ treatment. (F, G) The volume and weight in (E). (H) Immunohistochemical staining of Ki67 in tumor tissues. Scale bar, 50 μm. (*, P<0.05; **, P< 0.01; ***, P < 0.001).

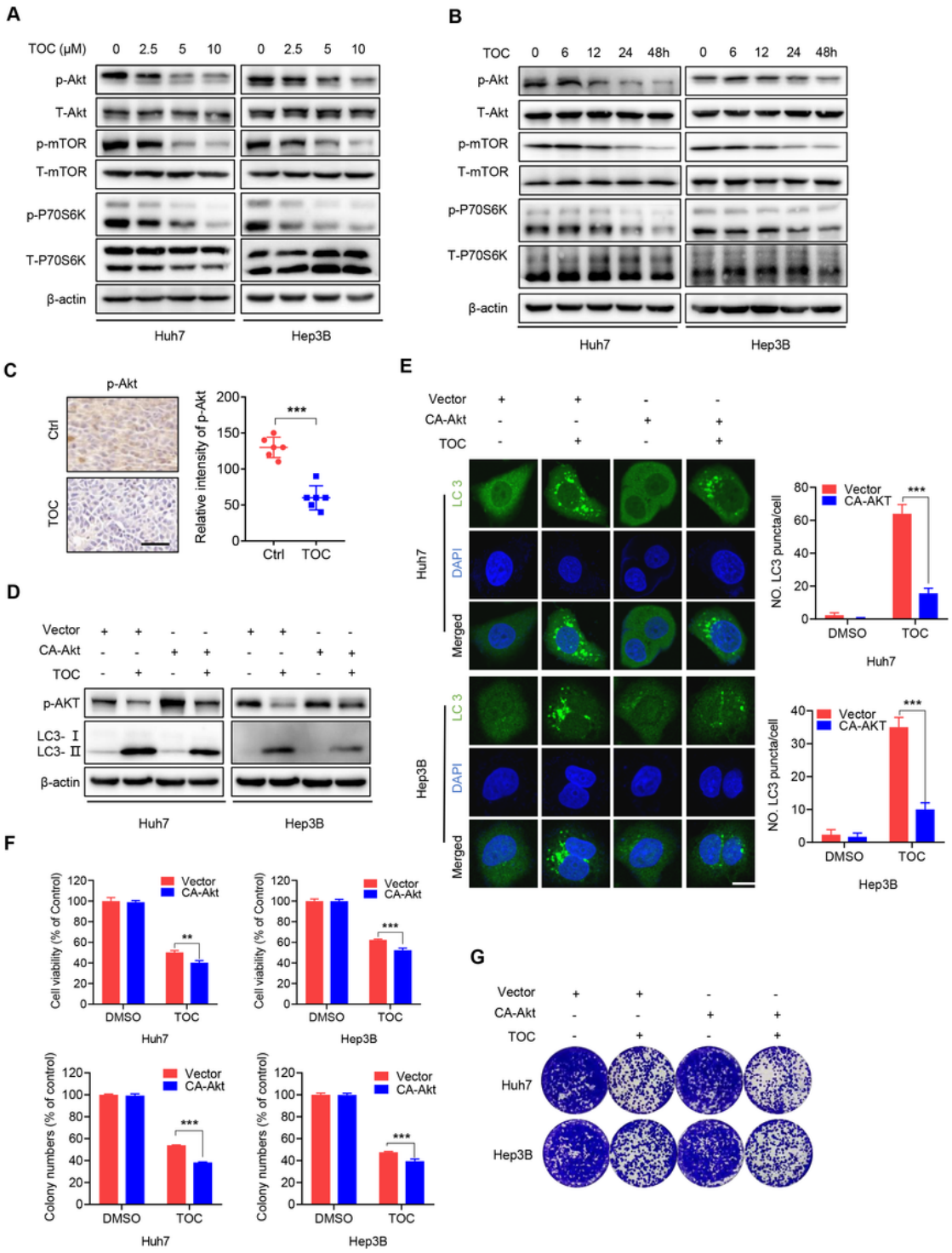

Figure 5

TOC induces autophagy by suppressing the Akt/mTOR pathway in HCC cells. (A, B) Immunoblotting analysis of Akt, mTOR, p70S6K, and their phosphorylated counterparts in Huh7 and Hep3B cells treated with indicated concentrations of TOC for 24 h (A), or 10μM TOC for indicated times (B). (C) Immunohistochemical staining of p-Akt in tumor tissues. Scale bar, 50 μm. (D) Immunoblotting analysis of LC3 in HCC cells transfected with empty vector or constitutively active CA-Akt for 24 h, followed by treatment with or without TOC (10 μM, 24 h). (E) Immunofluorescence analysis of LC3 in HCC cells treated as in (D). Scale bar, 20μm. (F) The MTT assay of HCC cells treated as in (D). (G) Colony formation assay of HCC cells treated as in (D). (*, P <0.05; **, P< 0.01; ***, P < 0.001).

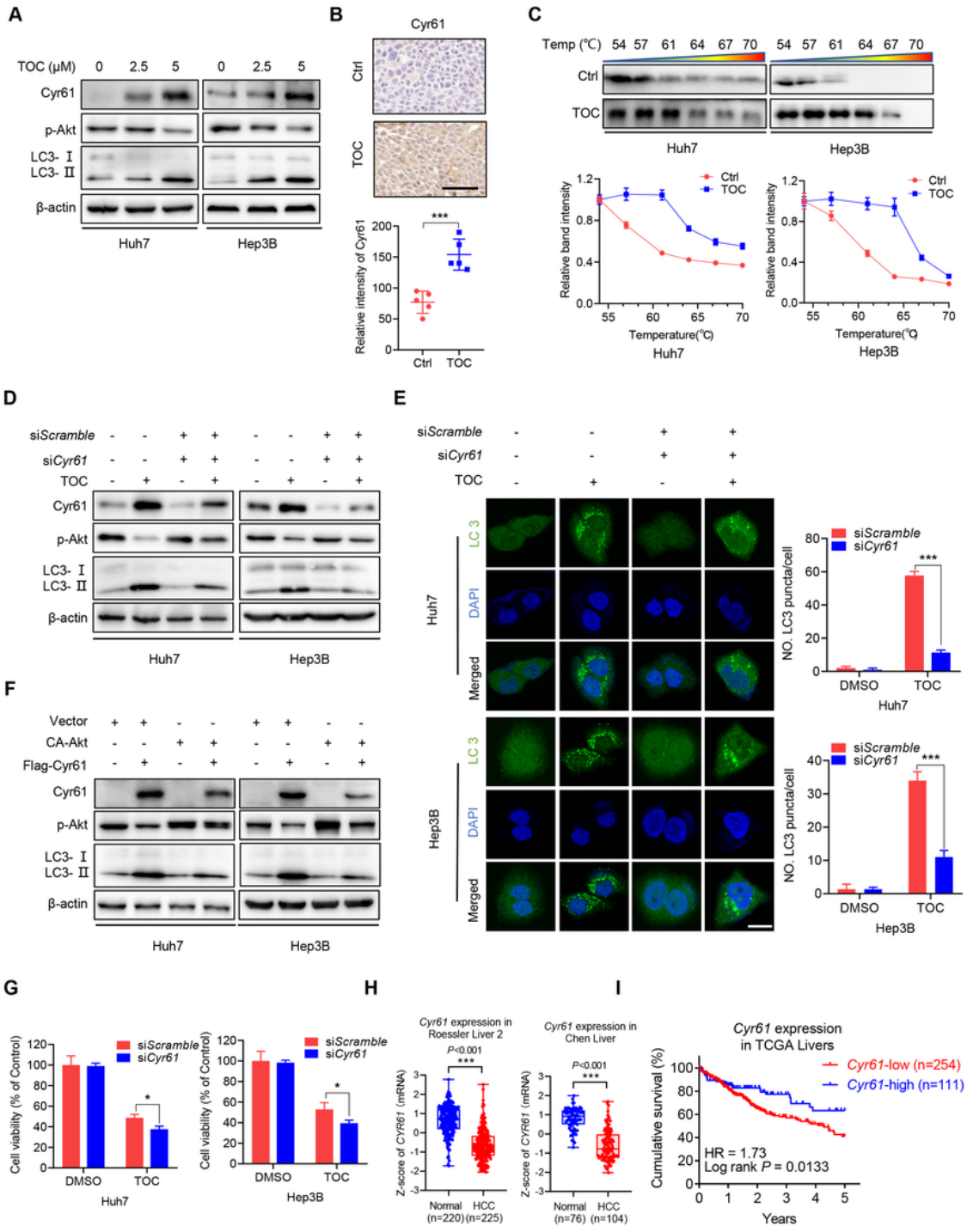

Figure 6

TOC initiates autophagy via Cyr61/Akt axis in HCC cells. (A) Immunoblotting analysis of Cyr61, phosphorylated Akt, and LC3 in Huh7 and Hep3B cells treated with indicated concentrations of TOC for 24 h. (B) Immunohistochemical staining of Cyr61 in tumor tissues. Scale bar, 50 μm. (C) Cellular thermal shift assay showing target engagement of CYR61 by TOC in Huh7 and Hep3B cells. (D) Immunoblotting analysis of Cyr61, phosphorylated Akt, and LC3 in HCC cells transfected with si*Scramble* or si*Cyr61* for 24

h, followed by treatment with or without TOC (10 μM, 24 h). (E) Immunofluorescence analysis of LC3 in HCC cells treated as in (C). Scale bar, 20μm. (F) Immunoblotting analysis of Cyr61, phosphorylated Akt, and LC3 levels in HCC cells co-transfected with Flag-Cyr61 and CA-Akt plasmids for 48 h. (G) The MTT assay of HCC cells treated as in (C). (H) Cyr61 mRNA expression in HCC tumors or non-tumor adjacent tissues according to Oncomine dataset (Rossier Liver 2 and Chen Liver). (I) Overall survival of HCC patients with high or low Cyr61 expression according to TCGA database. (*, P<0.05; **, P< 0.01; ***, P< 0.001).

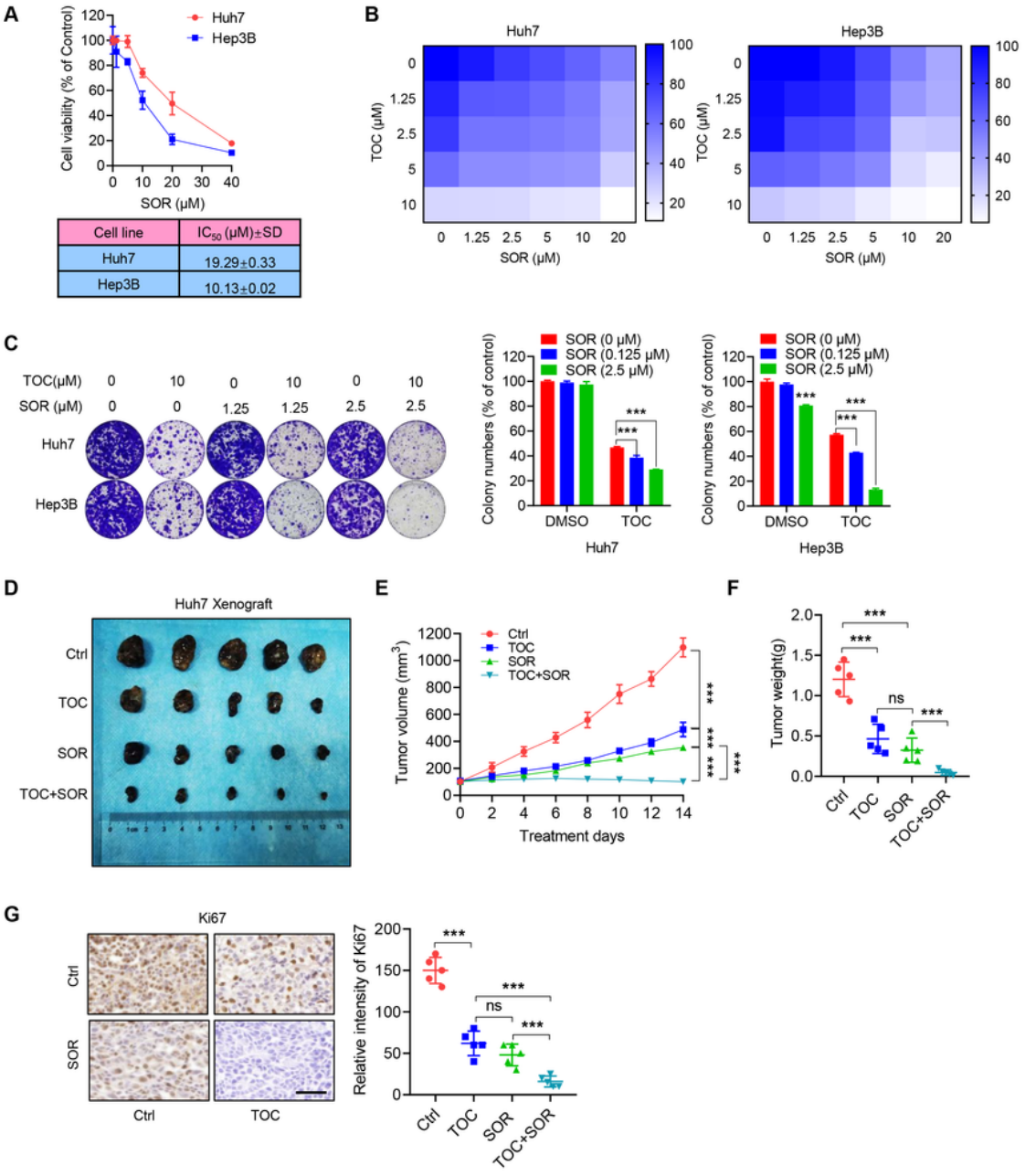

Figure 7

TOC enhances therapeutic response of HCC cells to sorafenib *in vitro* and *in vivo*. (A) MTT assay of Huh7 and Hep3B cells incubated with indicated concentrations of sorafenib for 24 h. (B) MTT assay of HCC cells treated with the indicated concentrations of TOC and sorafenib for 24 h. (C) Colony formation assay of HCC cells treated as in (B). (D) The images of isolated tumors derived from vehicle, TOC or sorafenib-treated mice. (E) The volume of individual tumors was measured at the indicated time points. (F) The weight of individual tumors in (D). (G) Immunohistochemical staining of Ki67 in tumor tissues. Scale bar, 50 μm. (*, P <0.05; **, P< 0.01; ***, P < 0.001).

Supplementary Files

This is a list of supplementary files associated with this preprint. Click to download.

- Supplementaryfigures.pdf
- FigureLegend.docx